Environ. Sci. Technol. **2004**, *38,* 3908−3915

Role of Dissolved Organic Matter, Nitrate, and Bicarbonate in the Photolysis of Aqueous Fipronil

SPENCER S. WALSE, STEPHEN L. MORGAN, LI KONG, AND JOHN L. FERRY*

Department of Chemistry and Biochemistry, University of South Carolina, Columbia, South Carolina 29208

A multivariate kinetic model of aqueous fipronil photodegradation was developed as a function of dissolved organic matter (DOM), bicarbonate, and nitrate at concentrations that bracket those commonly observed in natural waters (ca. 0−10 mg/L). Several pathways were available for fipronil photodegradation in this system, including direct photolysis and indirect photooxidation by species produced during the illumination of natural waters (e.g., ^{3}NOM*, $^1O_2$*, •OH, •CO_3^{1-}, •OOR, •OOH, e_{aq}^-, $O_2^{\bullet-}$). Product studies indicated that fipronil was quantitatively converted to fipronil desulfinyl, a product that is associated with direct photolysis alone. DOM was the only variable that affected fipronil degradation; it decreased the rate of fipronil photodegradation primarily through competitive light absorption (i.e., attenuation) and the quenching of fipronil*. The addition of sodium chloride (30‰) resulted in a more rapid rate (∼20%) of fipronil loss in comparison to equivalent experiments performed without sodium chloride, implying that fipronil may be more photolabile in marine environments.

Introduction

Fipronil [5-amino-1-[2,6-dichloro-4-(trifluoromethyl) phenyl]-4-[(trifluoromethyl) sulfinyl]-1*H*-pyrazole-3-carbonitrile], a phenylpyrazole insecticide, is widely used to control invertebrate pests (*1, 2*). The mechanism of fipronil toxicity, noncompetitive inhibition of the γ-aminobutyric acid (GABA) regulated chloride channel (*3, 4*), operates with similar efficacy for many invertebrates (*5*). Accordingly, runoff from sites of fipronil application can impact nontarget aquatic organisms (*1, 2, 6*), particularly crustaceans (*7−11*).

A photodegradation product, fipronil desulfinyl, is readily formed on crops (*12*), soils (*13, 14*), and in aqueous systems (*7, 15−19*) via photo-initiated sulfinyl extrusion [the result of a concerted rearrangement (*20*), or homolytic α-cleavage to form a sulfinyl/trifluoromethyl radical pair (*12, 21, 22*)] (Figure 1). Although the toxicity of fipronil and fipronil desulfinyl varies between different invertebrate species, in general fipronil and fipronil desulfinyl exhibit similar toxicity within a single species (*1, 2, 12*).

The photodegradation product may prove to be of greater environmental concern than fipronil itself. Although both have similar log K_{ow} values (fipronil, 4.01 (6), 3.56 (23); fipronil desulfinyl, 4.63) (*23, 24*)), volatilities (Henry's law constants (HLC) at 25 °C: fipronil desulfinyl, 1.6×10^{-8}; fipronil, 8.5×10^{-10}) (*18*), and solubilities (mg/L: fipronil, 1.6; fipronil desulfinyl, 0.4) (*23*), previous studies suggest that fipronil desulfinyl is less reactive than fipronil. Specifically, fipronil desulfinyl is stable toward photolysis on leaf surfaces (*12*), photolyzes only slowly in solution (*20*), and appears to be less susceptible toward hydrolysis than fipronil (*13, 14, 16, 18−20, 25*).

Previous research has identified DOM, NO_3^{1-}, and HCO_3^{1-}/CO_3^{2-} as significant participants in the photochemical degradation of hydrophobic organic micropollutants (HOMs) in surface waters; accordingly, identifying their effect on fipronil desulfinyl formation was of interest. Their contributions are a complex function of their absorption spectrum (with regard to its overlap with that of a given HOM and the available solar emission spectrum of 290−800 nm) and their reactivity with any subsequent photoinitiated reactive transients (e.g., ^{3}DOM* (*26−30*), $^1O_2$* (*29−34*), •OH (*35−40*), •CO_3^{1-} (*35, 41−43*), •OOR (*38, 44−46*), e_{aq}^- (*47−49*), $O_2^{\bullet-}$, and •OOH (*50, 51*)). The role these materials play in photochemical degradation is concentration dependent; since their concentrations in surface waters vary widely with geography and land-use patterns, their effects vary widely across different watersheds.

In this work, we expand on previous multivariate photodegradation studies (*52, 53*) by generating a predictive kinetic model in the laboratory for describing the fate of fipronil in surface waters of varying composition. The model was generated from measuring the effect of varying DOM, NO_3^{1-}, and HCO_3^{1-} (CO_3^{2-}) on the rate of aqueous fipronil photolysis at concentrations that bracket those commonly observed in surface waters throughout the Piedmont and Sandhill regions of the southeastern U.S. (*54*). We then tested that model against the results obtained from studying the degradation of fipronil in laboratory models of coastal plain surface water ("blackwater") and in estuarine mesocosms (*55−59*).

Experimental Section

Materials. Barnstead E-pure water (18 MΩ cm) was used for all solutions. OmniSolv GC^2 grade methyl *tert*-butyl ether (MTBE) was purchased from EM Science (Darmstadt, GR). 4-Bromoanisole (99+%) was acquired from Aldrich; NaCl, $NaNO_3$, and $NaHCO_3$ were used as received from Fischer Scientific. Freeze-dried Suwanee River natural organic matter was obtained from the International Humic Substances Society and was utilized as a generic representative of southeastern U.S. dissolved organic matter (DOM). DOM UV−vis absorption is featureless and decreases with increasing wavelength [UV−vis spectrum, Supporting Information (SI) Figure 1]. Crystalline $K_3Fe(C_2O_4)_3 \cdot 3H_2O$ was prepared by the method of Taylor (*60*), stored in the dark, and used for actinometric measurements. Fipronil (98%) was obtained from Chem Service (West Chester, PA). The syntheses, separation, and purification of fipronil and its related products, fipronil sulfide, fipronil sulfone, fipronil desulfinyl, and fipronil amide, were reported in a previous study by Walse et al. (*56*). All absorbance measurements were taken with a Cary 500 Scan UV−vis−NIR spectrophotometer.

Experimental Design. A four-factor central composite design, with five levels of each factor and six replicates of the center point, was employed for the multivariate analysis (*61, 62*). The four factors and their levels in the design are listed in Table 1. The design involved a total of 30 experiments run in a randomized order in three different blocks (see Table 4). The design and analysis was conducted using Design-Expert (version 5, Stat-Ease Inc., Minneapolis, MN). The modeled response (y) was the observable rate constant of fipronil photolysis ($k_{p\text{-obs}} \cong k_d$, vide infra), the negative slope obtained by linear least-squares analysis of ($\ln[fip]_t/[fip]_0$)

* Corresponding author phone: (803)777-2646; fax: (803)777-9521; e-mail: ferry@mail.chem.sc.edu.

10.1021/es0349047 CCC: $27.50 © 2004 American Chemical Society
Published on Web 06/05/2004

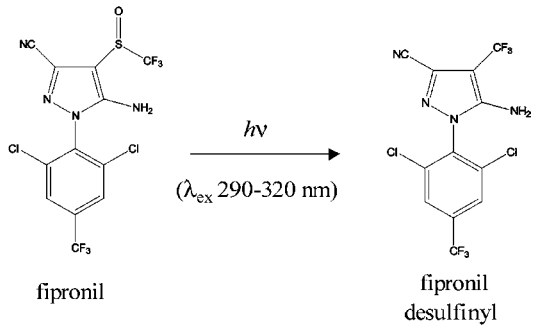

FIGURE 1. Fipronil desulfinyl is readily formed via photoinitiated sulfinyl extrusion from fipronil; direct photolysis appears to be the only route for the generation of this product.

TABLE 1. Factor Definitions, Coding Levels, and Design Points for the Four-Factor Central Composite Design

factor (original units)	factor levels				
x_1: fipronil concentration[a] (ng/L)	500	1000	1500	2000	2500
x_2: bicarbonate (HCO_3^-) concentration[a] (mg/L)	0	2.5	5	7.5	10
x_3: natural organic matter[a] (NOM) (mg/L)	0	2.5	5	7.5	10
x_4: nitrate (NO_3^-) concentration[a] (mg/L)	0	1	2	3	4

[a] Denotes initial concentrations.

TABLE 2. Analysis of Variance Table for the Response Surface Fitted to the Data from the Four-factor Design[a]

source	sum of squares	degrees of freedom (DF)	mean square	F value	prob > F
blocks	1.270×10^{-4}	2	6.349×10^{-5}		
model	0.011	14	7.518×10^{-4}	46.25	<0.0001
residual	2.113×10^{-4}	13	1.626×10^{-5}		
lack of fit	2.100×10^{-4}	10	2.100×10^{-5}	49.62	0.0041
pure error	1.270×10^{-6}	3	4.233×10^{-7}		
corrected total	0.011	29			

[a] The root-mean-square error of prediction was 4.032×10^{-3}, and the coefficient of determination (R^2) was 0.9803.

plotted versus time. The full second-order model with all possible two-factor interactions contained 15 parameters:

$$y = \beta_0 + \beta_1 x_1 + \beta_{11} x_1^2 + \beta_2 x_2 + \beta_{22} x_2^2 + \beta_3 x_3 + \beta_{33} x_3^2 + \beta_4 x_4 + \beta_{44} x_4^2 + \beta_{12} x_1 x_2 + \beta_{13} x_1 x_3 + \beta_{14} x_1 x_4 + \beta_{23} x_2 x_3 + \beta_{24} x_2 x_4 + \beta_{34} x_3 x_4 \quad (1)$$

where $x_1 - x_4$ represent the level of the four experimental factors (see Table 1). The parameters of this full second-order model in four factors include the following: β_0 represents a constant or offset term; $\beta_1, \beta_2, \beta_3, \beta_4$ estimate the linear effects of the four factors; $\beta_{11}, \beta_{22}, \beta_{33}, \beta_{44}$ estimate the quadratic (curvature) effects of the four factors; and $\beta_{12}, \beta_{13}, \beta_{14}, \beta_{23}, \beta_{24}, \beta_{34}$ estimate the interaction effects between every pair of two factors.

Experimental Procedure. $NaHCO_3$ (0.135 g/L), $NaNO_3$ (0.137 g/L), and DOM (0.1 g/L) stock solutions were diluted in a 100-mL volumetric flask to achieve the HCO_3^-, NO_3^-, and DOM concentrations outlined in the experiment design. The solution was then transferred to an airtight, modified 140-mL Pyrex hydrogenation vessel (Ace glass 7482-41), and continuously stirred with a Teflon-coated stir bar at 27 °C in the dark. pH was monitored (Orion 410A meter, Cole Parmer 05997-10 Ag/AgCl electrode) over a 60 min equilibration period and was maintained at 7.5 by the dropwise addition of either 0.01 M HCl or 0.01 M NaOH.

After equilibration, appropriate volumes of a 4.5×10^{-6} M fipronil stock (aqueous) were introduced to yield initial aqueous fipronil concentrations (nominal) of 500, 1000, 1500, 2000, or 2500 ng/L (ppt) (as outlined in the experiment design). These concentrations/conditions were chosen to emulate environmentally realistic concentrations of aqueous

TABLE 3. Parameter Estimates and Hypothesis Tests for the Parameters of the Full Second-Order Model Fitted to the Data[a]

parameter	estimate	DF	standard error	t for H_0: parameter = 0	prob > |t|
intercept	0.10	1	1.646×10^{-3}		
β_1, fipronil	-7.333×10^{-4}	1	8.230×10^{-4}	−0.89	0.3891
β_2, HCO_3^-	8.500×10^{-4}	1	8.230×10^{-4}	1.03	0.3205
β_3, DOM	−0.021	1	8.230×10^{-4}	−25.31	**<0.0001**
β_4, NO_3^-	-1.917×10^{-4}	1	8.230×10^{-4}	−0.23	0.8195
β_{11}	-1.183×10^{-3}	1	7.698×10^{-4}	−1.54	0.1482
β_{22}	-6.583×10^{-4}	1	7.698×10^{-4}	−0.86	0.4079
β_{33}	-1.333×10^{-4}	1	7.698×10^{-4}	−0.17	0.8652
β_{44}	-6.583×10^{-4}	1	7.698×10^{-4}	−0.86	0.4079
β_{12}	0.000	1	1.008×10^{-3}	0.000	1.0000
β_{13}	-5.000×10^{-4}	1	1.008×10^{-3}	−0.50	0.6281
β_{14}	-2.125×10^{-4}	1	1.008×10^{-3}	−0.21	0.8363
β_{23}	3.250×10^{-4}	1	1.008×10^{-3}	0.32	0.7522
β_{24}	-1.875×10^{-4}	1	1.008×10^{-3}	−0.19	0.8553
β_{34}	1.087×10^{-3}	1	1.008×10^{-3}	1.08	0.3002

[a] At the 95% level of confidence (i.e., $t < 0.05$), only a single factor effect, the linear dependence of $k_{p\text{-obs}}$ on DOM loading, was significantly different than zero.

TABLE 4. Listing of Experimental Parameters, Order in Which the Experiments Were Performed, and Observed Rate Constants of Fipronil Photodegradation that Were Used To Develop Our Kinetic Model

run	block	fipronil (ng/L)	DOM (mg/L)	HCO_3^{1-} (mg/L)	NO_3^{1-} (mg/L)	$k_{p\text{-obs}} \cong k_d$ (min^{-1})	r^2 [a]	(n)	m.b.[b]
1	1	2000	2.5	2.5	1	0.1165	0.99	7	94
2	1	2000	2.5	7.5	3	0.0794	0.97	8	97
3	1	1000	7.5	2.5	1	0.1125	0.96	7	89
4	1	1000	7.5	7.5	3	0.0788	0.98	7	98
5	1	2000	7.5	2.5	3	0.1136	0.97	8	98
>6[c]	1	1500	5	5	2	0.0996	0.98	8	93
>7	1	1500	5	5	2	0.1011	0.98	8	98
8	1	1000	2.5	2.5	3	0.115	0.94	7	99
9	1	2000	7.5	7.5	1	0.0747	0.92	9	93
10	1	1000	2.5	7.5	1	0.0752	0.94	7	98
11	2	2000	2.5	2.5	3	0.1115	0.99	9	92
>12	2	1500	5	5	2	0.1007	0.97	8	97
13	2	1000	2.5	2.5	1	0.1201	0.96	7	92
14	2	1000	2.5	7.5	3	0.0753	0.98	8	93
15	2	1000	7.5	7.5	1	0.0784	0.98	8	93
>16	2	1500	5	5	2	0.1005	0.99	8	93
17	2	1000	7.5	2.5	3	0.1172	0.98	7	99
18	2	2000	2.5	7.5	1	0.0695	0.96	9	99
19	2	2000	7.5	2.5	1	0.1185	0.98	8	98
20	2	2000	7.5	7.5	3	0.0714	0.96	9	95
21	3	1500	10	5	2	0.1057	0.98	8	98
>22	3	1500	5	5	2	0.0989	0.96	8	98
23	3	1500	0	5	2	0.0968	0.97	8	99
24	3	1500	5	0	2	0.1478	0.96	7	98
25	3	2500	5	5	2	0.0991	0.99	11	95
26	3	1500	5	5	4	0.1009	0.99	11	98
27	3	1500	5	10	2	0.0589	0.96	11	94
>28	3	1500	5	5	2	0.0994	0.98	11	93
29	3	1500	5	5	0	0.1016	0.98	10	96
30	3	500	5	5	2	0.0992	0.98	10	95

[a] Coefficient of determination for $(\ln[\text{fipronil}]_t/[\text{fipronil}]_0)$ plotted versus t (min^{-1}). [b] Mass balance (fipronil desulfinyl yield as % fipronil loss). [c] > indicates center point" experiment.

fipronil that could enter the aquatic environment via runoff, vapor deposition, or spray drift (*63*). Fipronil stock solution was stored at 4 °C in the dark; hydrolysis or photolysis of fipronil was not observed in the stock solution. The resulting solution was allowed to equilibrate for 15 min with rapid mixing. A sample was then withdrawn to determine the initial concentration (actual) of fipronil before the solution was irradiated (λ_{ex} = 290−800 nm) with a 1000 W Xe arc lamp. Solution temperature averaged 29 ± 2 °C. Duplicate experiments were performed in the dark to investigate the contribution of thermal processes toward fipronil loss (av 29 ± 2 °C).

For quantification, samples (1.5 mL) were removed from the reactor through an airtight Teflon sampling port with a spring-loaded 4-mL Manostat syringe. Samples were immediately placed in Fisherbrand 20-mL amber EPA vials precharged with 1.5 mL of chilled MTBE + internal standard (4-bromoanisole). The samples were then rapidly mixed for 2 min on a vortex Genie mixer; emulsions were broken by the addition of ∼100 mg of NaCl. MTBE extracts were transferred by a Pasteur pipet to 11-mm amber crimp-top GC vials and stored at 4 °C for later analysis by gas chromatography with electron capture detection (GC-ECD; HP 5890).

At the conclusion of each experiment, the remaining solution was extracted with 2 × 50 mL of MTBE. The MTBE extracts were dried with anhydrous $MgSO_4$, concentrated to ∼2 mL, transferred to GC vials as described, and used for qualitative product determination by gas chromatography with ion trap mass spectrometric detection (GC-ITMS).

Extraction efficiencies (quadruplicate) from fortified aqueous solutions at pH 7.5 and 25 mg/L DOM were measured 50 min after substrate addition and are reported as average values: fipronil, 97.6 ± 0.7%; fipronil desulfinyl, 98.6 ± 0.5%; fipronil sulfide, 98.5 ± 0.7; fipronil sulfone, 95.9 ± 0.5%; and fipronil amide, 90.7 ± 0.5%.

Products were verified by matching retention times and electron impact (EI) mass spectra against those of purchased or synthesized standards. Chromatographic conditions and method detection limits for all analytes (GC-ECD and GC-ITMS) were reported previously by Walse et al. (*56*). The retention times, R_T's, of the fipronil analytes are presented in Supporting Information (SI Table 1) as are their mass spectra (SI Figures 2−6). The standard deviation associated with triplicate injections was used to assess error in all GC concentration measurements.

Solar Simulation. A 1000 W Xe arc lamp (Oriel PN-1331369) with an Oriel (Stratford, CT) 68820 power supply and 66021 lamp housing was used for polychromatic irradiation (SI Figure 7) (*64*). The lamp housing was equipped with a 10-cm long Pyrex water-cooled IR filter to limit the spectral output, λ_{ex}, to 290−800 nm. The average incident light intensity (I_{av}), over the wavelengths of fipronil absorption (290−320 nm), was 7.41×10^{16} photons cm^{-3} s^{-1}. This light source was allowed to stabilize for 20 min prior to use.

Monochromatic Irradiation (310 nm). An Osram (HBO 103 W/2) 100 W Hg short arc lamp with a Photon Technology International (New Brunswick, NJ) A-1010B lamp housing, 220B power supply, and a 101 grating monochromator was used as a source of monochromatic light. Slits were set at 0.6 mm with a ±2.4 nm band-pass (SI Figure 8) (*65*). The incident light intensity just within the photolysis cell front window ($I_0^i = 7.4 \times 10^{-7}$ Einstein min^{-1}) was measured by ferrioxalate actinometry as described by Calvert and Pitts (*66*). This light source was allowed to stabilize for at least 30 min prior to use.

Results and Discussion

Quantum Yield and Path Length Determinations. Utilizing ferrioxalate as a high optical density actinometer (*67*), the quantum yield of direct fipronil photolysis, ϕ_D, was determined to be 1.3×10^{-4}. We observed good agreement between quantum yield measured as a function of fipronil loss and fipronil desulfinyl formation ($\phi_{d\text{-fipronil-loss}}/\phi_{d\text{-fip-desulfinyl-formation}}$ = 0.92 ± 6%). The effective path length, *l*, of the reaction vessel was determined to be 1.4 cm by the method of Zepp (*68*). Both calculations required the use of monochromatic irradiation (vide supra).

Multivariate Photolysis Study: Kinetic Description of Fipronil Loss. Fipronil was quantitatively recovered (>95%) in all dark controls, indicating that nucleophilic addition to DOM (1,2 and 1,4) (*69*), hydrolysis, sulfinyl oxidation (*18, 20*), volatilization, and sorption onto reactor walls were not significant contributors toward fipronil loss in the photolysis experiments.

The loss of fipronil upon polychromatic irradiation (λ_{ex} = 290−800 nm) was apparently first order in fipronil and could be described by the differential rate equation

$$-(d[\text{fipronil}]_{aq}/dt)_p = k_{p\text{-obs}}[\text{fipronil}]_{aq} \quad (2)$$

where the observable rate constant of photolysis across all wavelengths, $k_{p\text{-obs}}(min^{-1})$, is defined as

$$k_{p\text{-obs}} = k_d + k_i \quad (3)$$

that includes the first-order direct, k_d (min^{-1}), and indirect, k_i (min^{-1}), photoreaction rate constants. Experimental data supported this kinetic model; plots of $(\ln[\text{fipronil}]_t/[\text{fipronil}]_0)$ versus time were linear (SI Figure 9), indicating that overall fipronil photolysis displayed first-order kinetics under all experimental conditions. The rate constant, $k_{p\text{-obs}}$ (min^{-1}), is the negative of the slope obtained by a linear least-squares analysis and has a value of 0.1003 ± 0.0009 (n = 6) at the experimental center point (1500 ng/L fipronil, 5 mg/L (ppm) DOM, 5 mg/L HCO_3^{1-}, and 2 mg/L NO_3^{1-}).

The analysis of variance for the fit of the full second-order model to the data from the four-factor central composite design is shown in Table 2. The coefficient of multiple determination, R^2, for the fit of the model to the experimental data was 0.9803; i.e., 98% of the variation in the data about its mean was accounted for by the factor effects in the model. Although lack of fit of the full second-order model is significant ($p \geq 0.0050$), plots of residuals do not show any significant trends. The only factor effect that was significantly different from zero at the 95% level of confidence (i.e., student's $t < 0.05$) was the linear effect of DOM (noted in bold font in Table 3) (SI Figures 10−12). The block effect (related to time) was also not significant at the 95% level of confidence. Nitrate did not appear to affect the rate of fipronil removal under our conditions, probably because of preferential reaction of photogenerated hydroxyl radicals with DOM or HCO_3^{1-}/CO_3^{2-} (*35, 37, 40, 52, 53*).

A model containing only two parameters, an intercept ($k_{p\text{-obs}}$) and DOM loading, was then fitted to the data. The resulting coefficient of determination, r^2, was 0.9589; i.e., 96% of the variation in the data about its mean was attributed to the inverse relationship (linear) between DOM loading and the rate of fipronil photodegradation (Figure 2). However, DOM did not affect the product profile associated with fipronil photodegradation. Product analysis (quantitative and qualitative) identified fipronil desulfinyl as the only product in these experiments; its formation accounted for ∼89−95% of fipronil loss over all the experiments (Figure 3; Table 4).

These observations suggest that indirect photochemical processing of fipronil by DOM and nitrate are not significant for natural surface waters bracketed by these experimental conditions. Similar observations have been reported by Miller and Zepp (*70−73*) in studies on HOMs that experience direct photolyses (i.e., $k_d \gg k_i$).

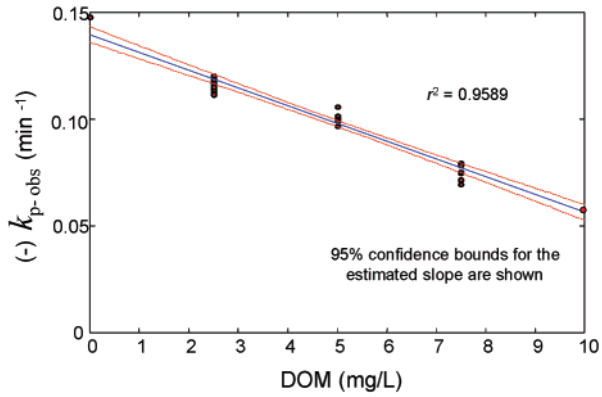

FIGURE 2. 96% ($r^2 = 0.9589$) of the variation in the data about its mean was attributed to the inverse relationship (linear) between DOM loading and the rate of fipronil photodegradation.

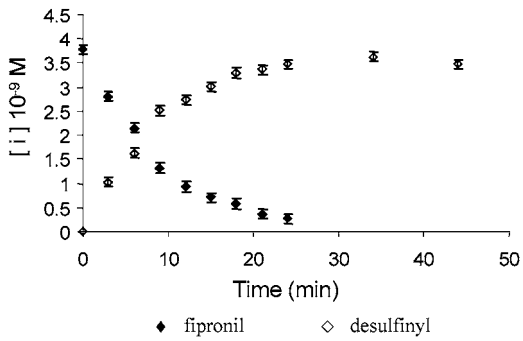

FIGURE 3. Loss of aqueous fipronil upon irradiation ($\lambda_{ex} = 290-800$ nm) is illustrated for run 11 (2000 ng/L fipronil, 2.5 mg/L HCO_3^{1-}, 2.5 mg/L DOM, and 3 mg/L NO_3^{1-}); similar quantitative conversion to fipronil desulfinyl, via direct sulfinyl extrusion, was observed in every experiment (mass balance ($\bar{x} \pm s$) 92.5 ± 0.6%).

Under that condition, eq 2 reduces to

$$-(\mathrm{d}[\text{fipronil}]_{\mathrm{aq}}/\mathrm{d}t)_{\mathrm{d}} = k_{\mathrm{d}}[\text{fipronil}]_{\mathrm{aq}} \tag{4}$$

where k_{d} represents the observable rate constant for fipronil loss during polychromatic irradiation (290−320 nm, SI Figure 13) and $\cong k_{\text{p-obs}}$ (Table 4). The rate of fipronil loss (eq 4) can also be expressed as:

$$\text{rate} = -(\mathrm{d}[\text{fipronil}]_{\mathrm{aq}}/\mathrm{d}t)_{\mathrm{d}} = -\sum_{\lambda(290-320\ \mathrm{nm})} (\mathrm{d}[\text{fipronil}]_{\mathrm{aq}}/\mathrm{d}t)_{\mathrm{d}\lambda}$$

$$= \phi_{\mathrm{d}} \sum_{\lambda(290-320\ \mathrm{nm})} I^{\mathrm{d}}_{\mathrm{a}\lambda} \tag{5}$$

where ϕ_{d} is the wavelength-independent quantum yield and $I^{\mathrm{d}}_{\mathrm{a}\lambda}$ (photons cm^{-3} s^{-1}) is the intensity of light absorbed by fipronil at a fixed wavelength λ, given by (*67, 74*)

$$I^{\mathrm{d}}_{\mathrm{a}\lambda} = I_{\lambda} F_{\mathrm{s}\lambda} F_{\mathrm{c}\lambda} \tag{6}$$

where I_{λ} is the incident light intensity (photons cm^{-3} s^{-1}). The system ($F_{\mathrm{s}\lambda}$) and fipronil ($F_{\mathrm{c}\lambda}$) fractional absorbance (dimensionless) are defined by eqs 7 and 8, respectively, derived from the Beer−Lambert Law:

$$F_{\mathrm{s}\lambda} = \{1 - 10^{-(\alpha_{\lambda} + \epsilon_{\lambda\text{-fip}}[\mathrm{fip}]_{\mathrm{aq}} + \epsilon_{\lambda\text{-NO}_3{}^{1-}}[\mathrm{NO_3}^{-1}])l}\} \tag{7}$$

$$F_{\mathrm{c}\lambda} = \frac{\epsilon_{\lambda\text{-fip}}[\mathrm{fip}]_{\mathrm{aq}}}{\alpha_{\lambda} + \epsilon_{\lambda\text{-fip}}[\mathrm{fip}]_{\mathrm{aq}} + \epsilon_{\lambda-\mathrm{NO}_3{}^{1-}}[\mathrm{NO_3}^{1-}]} \tag{8}$$

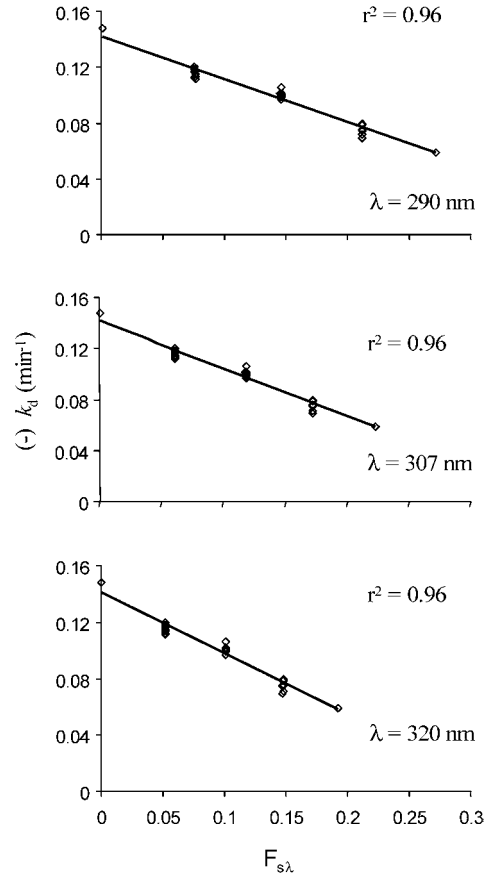

FIGURE 4. Over the absorption region of fipronil (290−320 nm), the strong linear correlation ($r^2 = 0.96$) between the (−) rate of direct photolysis (k_{d}) and the fraction of light absorbed by the system ($F_{\mathrm{s}\lambda}$) provides evidence that the attenuation of incident light affected fipronil photodegradation under conditions bracketed by these experiments.

where α_{λ} is the attenuation coefficient of DOM (cm^{-1}), and $\epsilon_{\lambda\text{-fip}}$ and $\epsilon_{\lambda\text{-NO}_3{}^{1-}}$ (M^{-1} cm^{-1}) (*75*) represent the respective molar absorptivities of fipronil and NO_3^{1-}. Carbonate and bicarbonate do not readily absorb between 290 and 800 nm and were omitted. Attenuation (α_{λ}) is directly proportional to DOM loading, over the range used in this study, from 290 to 320 nm (SI Figure 14). Under our experimental conditions, $\alpha_{\lambda} \gg \epsilon_{\lambda}[\mathrm{fip}]_{\mathrm{aq}} \gg \epsilon_{\lambda}[\mathrm{NO_3}^{1-}]_{\mathrm{aq}}$, it was not surprising to find that the intensity of light absorbed by fipronil ($I^{\mathrm{d}}_{\mathrm{a}\lambda}$), and ultimately the direct photolysis rate constant of fipronil (k_{d}), had a negative linear correlation ($r^2 = 0.96$) with the light absorbed by the system over the wavelengths 290−320 nm (the $F_{\mathrm{s}\lambda}$ term) (Figure 4). These results imply that fipronil desulfinyl formation would be inversely related to DOM loading in natural surface waters with less than 10 mg/L DOM.

However, the ability of DOM to inhibit direct fipronil photolysis was not exclusively due to attenuation. The effect of light attenuation on photolysis was predicted by calculating a "light screening factor", $\hat{S}_{\lambda}$, that is defined as the ratio of the intensity of light absorbed by fipronil with the attenuator present (i.e., with DOM) over the intensity of light absorbed by fipronil without the attenuator present (i.e., without DOM) (*67, 72, 73*):

$$\hat{S}_{\lambda} = \frac{\hat{I}^{\mathrm{d}}_{\mathrm{a}\lambda\text{-DOM}}}{\hat{I}^{\mathrm{d}}_{\mathrm{a}\lambda\text{-NO-DOM}}} \tag{9}$$

Substituting eqs 6−8 into eq 9 yields (*67*)

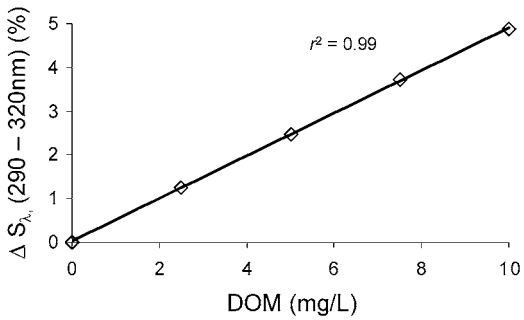

FIGURE 5. For every experiment, the "light screening fator" ($\hat{S}_\lambda$) was calculated and was found to be stable (within 5%) over 290–320 nm (i.e., DOM competed for incident light approximately equally over the wavelengths that fipronil absorbed).

$$\hat{S}_\lambda = \frac{1 - 10^{-(\alpha_\lambda + \epsilon_{\lambda\text{-fip}}[\text{fip}]_{\text{aq}} + \epsilon_{\lambda\text{-NO}_3^{1-}}[\text{NO}_3^{1-}])l}}{2.303\,(\alpha_\lambda + \epsilon_{\lambda\text{-fip}}[\text{fip}]_{\text{aq}} + \epsilon_{\lambda\text{-NO}_3^{1-}}[\text{NO}_3^{1-}])l} \quad (10)$$

assuming $\alpha_\lambda \gg \epsilon_\lambda[\text{fip}]_{\text{aq}} \gg \epsilon_\lambda[\text{NO}_3^{1-}]_{\text{aq}}$, this simplifies to

$$\hat{S}_\lambda \cong \frac{1 - e^{-(2.303\alpha_\lambda)l}}{2.303\alpha_\lambda l} \quad (11)$$

For every experiment, $\hat{S}_\lambda$ was calculated and was found to be stable (within 5%) over 290–320 nm (i.e., DOM competed for incident light approximately equally over the wavelengths that fipronil absorbed) (Figure 5 and SI Figure 15). Accordingly, $\hat{S}_\lambda$ estimates the theoretical effect of light attenuation over the entire range of wavelengths (290–320 nm), $\sum_{\lambda(290-320\text{nm})} \hat{S}_\lambda$. From eq 9, it can be seen that $\hat{S}_\lambda$ also estimates the ratio of the intensity of light absorbed by fipronil with DOM present over the intensity of light absorbed by fipronil without DOM from 290 to 320 nm:

$$\hat{S}_\lambda \cong \sum_{\lambda(290-320\text{nm})} \hat{S}_\lambda = \sum_{\lambda(290-320\text{nm})} \frac{\hat{I}^d_{\text{a}\lambda\text{-DOM}}}{\hat{I}^d_{\text{a}\lambda\text{-NO-DOM}}} \quad (12)$$

Expressing eq 12 in terms of eqs 4 and 5 yields

$$\hat{S}_\lambda \cong \frac{\hat{k}_{\text{d-DOM}}}{\hat{k}_{\text{d-NO DOM}}} \quad (13)$$

and provides justification to use $\hat{S}_\lambda$ as an approximation of the effect of light attenuation by DOM on photolysis kinetics in this study.

The observed "light screening factor", S, was solved for by inserting experimentally determined values for k_d and $k_{\text{d-NO-DOM}}$ into eq 13. It was consistently lower than $\hat{S}_\lambda$ across all experiments (i.e., $S/\hat{S}_\lambda$ was <1); indicating that the rate of fipronil photolysis was inhibited or quenched to a greater extent than would be predicted from light attenuation by DOM alone.

For each experiment, we determined quenching factors, Q_λ's, where (*67, 72, 73*)

$$Q_\lambda = 1 - (S/\hat{S}_\lambda) \quad (14)$$

The quenching (inhibition) of direct fipronil photolysis (Q_λ) was found to be directly proportional ($r^2 > 0.95$) to DOM loading (independent of its attenuation effect) and yielded the following empirical relationship

$$Q_\lambda = 0.04 + (0.05)\,[\text{DOM (mg/L)}] \quad (15)$$

that was effectively constant (within 5%) over all wavelengths of fipronil absorption (290–320 nm) (Figure 6).

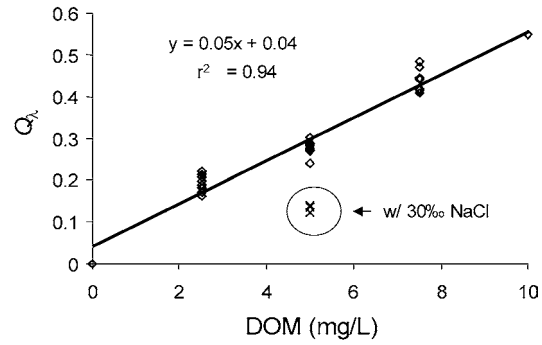

FIGURE 6. Independent of the effect of DOM light attenuation, quenching factors, Q_λ's, had a strong linear correlation ($r^2 = 0.94$) with DOM loading. Deviation from this empirical relationship was only observed in "center point" experiments in which 30‰ NaCl was introduced prior to substrate addition.

Two mechanisms are proposed to account for this phenomenon: collisionally induced nonradiative energy or electron transfer from fipronil* to DOM (i.e., dynamic quenching), or inhibition of fipronil* formation through complexation of the ground-state molecule (i.e., static quenching). Static quenching may be derived from binding of ground-state fipronil by DOM (sorption) (*76–81*). The fraction of total fipronil that is "free" (not sorbed to DOM), $\hat{f}_W$, can be used to estimate the relative contributions of static and dynamic quenching on the rate of fipronil photolysis (*40*):

$$-(\text{d}[\text{fipronil}]_{\text{aq}}/\text{d}t)_{\text{d}} = \hat{k}_{\text{SQ}}[\text{fipronil}]_{\text{aq}} = (\hat{S}_\lambda k_{\text{d-NO-DOM}}\,\hat{f}_W)[\text{fipronil}]_{\text{aq}} \quad (16)$$

where $\hat{k}_{\text{SQ}}$ is the rate constant of fipronil photolysis (predicted maximum), and

$$\hat{f}_W = \frac{1}{1 + [\text{DOM (kg/L)}]\hat{K}_{\text{OM}}(\text{L kg C}^{-1})} \quad (17)$$

An estimated value of $\hat{K}_{\text{OM}}$(L kg C^{-1}), the organic matter–water partition coefficient, was calculated using the method of Karickhoff (*82*):

$$\log \hat{K}_{\text{OM}} \cong 0.82 \log K_{\text{OW}} + 0.14 \quad (18)$$

The predicted rate constant ($\hat{k}_{\text{SQ}}$) represented only a fraction (log $K_{\text{ow}} = 4.01$, 30%; log $K_{\text{ow}} = 3.56$, 15%) of the observed rate (i.e., $\hat{k}_{\text{SQ}}/k_d \gg 1$), suggesting that dynamic quenching of fipronil* by DOM may make a larger contribution toward the inhibition of direct fipronil photolysis in this system than static. Several previous studies of HOM photodegradation in the presence of DOM support this interpretation (*52, 83*).

Additional quenching (inhibitory) effects on the rate of fipronil photodegradation were quantified by calculating the wavelength and DOM-loading independent quenching constant, k_Q(L mg^{-1} min^{-1}), where

$$k_{\text{Q}} = (-)\frac{k_{\text{d}} - (\hat{S}_\lambda k_{\text{d-NO-DOM}}\,\hat{f}_W)}{[\text{DOM (mg/L)}]} \quad (19)$$

Using "light screening factors" ($\hat{S}_\lambda$) calculated at 290, 307, and 320 nm, an average value of $7.9 \pm 1.1 \times 10^{-3}$ (estimate ± standard error) was obtained for k_Q (L mg^{-1} min^{-1}) across all DOM loadings. A one-way analysis of variance based on pooled standard deviations indicated that values of k_Q were statistically equivalent at 5, 7.5, and 10 mg/L DOM (95% confidence level); at 2.5 mg/L DOM the average value of k_Q was significantly higher at the 95% level of confidence

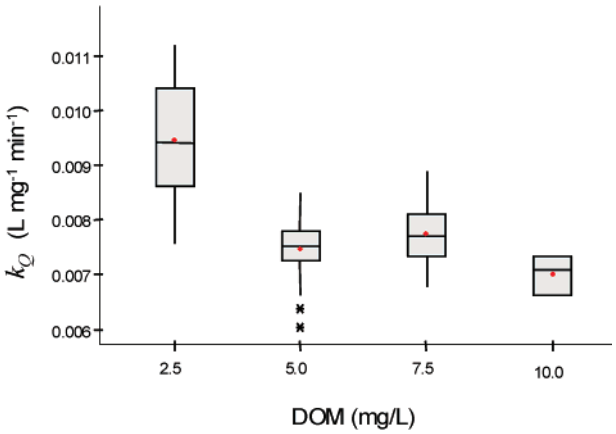

FIGURE 7. At the 95% level of confidence, a one-way analysis of variance based on pooled standard deviations indicated that values of k_Q were statistically equivalent at 5, 7.5, and 10 mg/L DOM; at 2.5 mg/L DOM the average value of k_Q was slightly higher ($9.4 \pm 1.0 \times 10^{-3}$).

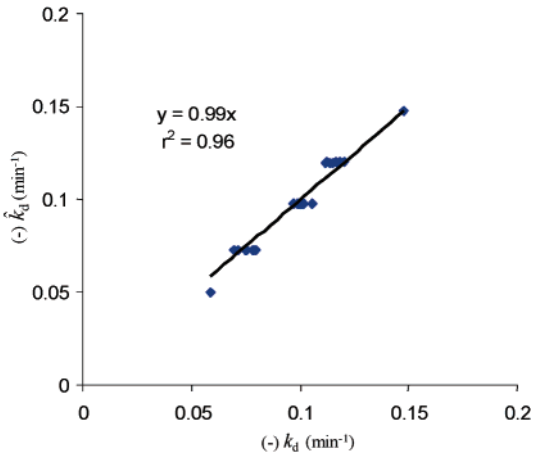

FIGURE 8. Predicted rates of fipronil photolysis, $\hat{k}_d$, were in good agreement with the observed rates, k_d (even at 2.5 mg/L DOM).

($9.4 \pm 1.0 \times 10^{-3}$) compared to the results at 5, 7.5, and 10 mg/L (Figure 7 and SI Table 2).

Substitution of eq 19 into eq 4 provided an overall kinetic description of fipronil photodegradation in this study:

$$-(\mathrm{d}[\text{fipronil}]_{\mathrm{aq}}/\mathrm{d}t)_{\mathrm{d}} = ((\hat{S}_\lambda k_{\text{d-NO-NOM}}\,\hat{f}_{\mathrm{W}}) - (k_{\mathrm{Q}}[\text{DOM (mg/L)}]))[\text{fipronil}]_{\mathrm{aq}} \quad (20)$$

At all DOM loadings, predicted rates of fipronil photolysis, $\hat{k}_d$, were within 8% of the observed rates (k_d's) (Figure 8).

Three replicates of the experimental center point were made at 30‰ NaCl to approximate the salinity of marine environments (seawater ≈ 35‰). At this NaCl loading, values of α_λ from 290 to 320 nm changed minimally (<3%) in comparison to the values without added NaCl (i.e., $\hat{S}_{\lambda\text{-NaCl}} \cong \hat{S}_\lambda$). In these experiments, the observed rate of fipronil removal ($k_{\text{p-obs}}$) increased approximately 20% to 0.1204 ± 0.0013 ($n = 3$) from the center point value of 0.1003 ± 0.0009 ($n = 6$) (Table 5). These results suggest that fipronil desulfinyl formation would increase in surface waters as fipronil is transported from riverine to marine systems. The rate increase corresponds to a reduction of the values of Q_λ and k_Q by approximately 50% (Figures 6, 9). This study was not designed to test for the mechanism of salt effects; however, possible explanations are a decrease in the degree of sorption required for the static quenching of HOMs* by DOM (*76, 77, 84−86*), a decrease in the dynamic quenching

TABLE 5. Listing of the Observed Rate Constants of Fipronil Photodegradation Used To Test Our Kinetic Model

run	conditions[a]	$k_{\text{p-obs}}$ (min^{-1})	r^2 [b]	(n)	m.b.[c]
31	5 mg/L DOM + 30 ‰ NaCl	0.1201	0.98	9	99
32		0.1193	0.97	9	96
33		0.1219	0.99	9	95
34	15 mg/L DOM	0.0426	0.92	8	84
35		0.0415	0.92	8	81
36		0.0449	0.91	8	82
37	20 mg/L DOM	0.0254	0.90	9	77
38		0.0237	0.92	9	71
39		0.0218	0.90	9	74
40	25 mg/L DOM	0.0112	0.88	10	65
41		0.0118	0.87	10	70
42		0.0123	0.89	10	72

[a] Center point concentrations of fipronil, HCO_3^{1-}, and NO_3^{1-} were in runs 31−42. [b] Coefficient of determination for ($\ln[\text{fipronil}]_t/[\text{fipronil}]_0$) plotted versus t (min^{-1}). [c] Mass balance (fipronil desulfinyl yield as % fipronil loss).

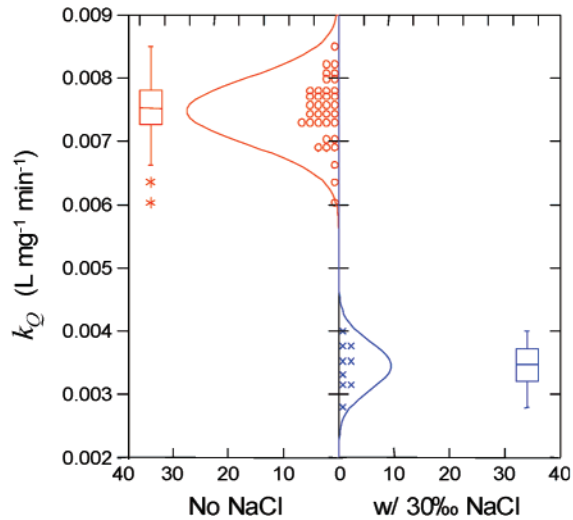

FIGURE 9. In three replicates of the experimental center point (1500 ng/L fipronil, 5 mg/L HCO_3^{1-}, 5 mg/L DOM, and 2 mg/L NO_3^{1-}) in which 30‰ NaCl was introduced prior to substrate addition, values of k_Q were reduced ~50%.

of HOMs* by DOM, or at least fipronil*, or a more efficient conversion of ^{1}fipronil to ^{3}fipronil.

A study by Walse et al. (*56*) reported the loss of aqueous fipronil in three replicate estuarine mesocosms having conditions typical of those found in the coastal regions and tidal creeks of the southeastern U.S. (salinity 20‰, 5 mg/L DOC, $I_{\text{av(290−320nm)}} \cong 2.0 \times 10^{14}$ photons cm^{-3} s^{-1}) (*58, 59*). Relative rate versus depth profiles (*78*) were developed (SI Figures 16−17), using eq 20, to predict the photolysis half-life of aqueous fipronil within the mesocosms ($t_{1/2\text{-max}}$, $k_Q = 7.9 \times 10^{-3}$ (without NaCl); $t_{1/2\text{-min}}$, $k_Q = 3.4 \times 10^{-3}$ (30‰ NaCl)). Although there are many uncertainties associated with laboratory-to-environment extrapolation, the estimated minimum ($t_{1/2} = 3.3 \pm 0.4$ day) and maximum ($t_{1/2} = 4.2 \pm 0.5$ day) values agree well with the observed half-lives (3.4 ± 0.8, 3.6 ± 0.7, 2.3 ± 0.9 day) over the initial 96 h of the mesocosm study (measured from $\mathrm{d}[\text{fipronil desulfinyl}]_{\mathrm{aq}}/\mathrm{d}t$).

Equation 20 predicts that fipronil photolysis will not be observed when the DOM loading exceeds ~16 mg/L, yet in experiments performed (triplicate) in which 15, 20, and 25 mg/L DOM was added to experimental center point concentrations of fipronil, NO_3^{1-}, and HCO_3^{1-} (CO_3^{2-}), we

observed fipronil photodegradation (Table 5). Although the quenching factors, Q_λ's, were consistent with the empirical relationship defined in eq 15, the quenching constants (k_Q's) decreased with DOM loading, representing only ~63%, 56%, and 46%, respectively, of the model derived average (7.9×10^{-3}). We have interpreted these observations to be a result of an increasing contribution of indirect fipronil photodegradation (accelerating effect) stemming from these higher DOM loadings. In addition to the work of Skurlatov et al. (*72*) that reported similar findings, a reduction in the percentage of fipronil loss represented by fipronil desulfinyl (15 mg/L, ~82%; 20 mg/L, ~74%; 25 mg/L, ~69%) provides support for this interpretation and suggests a similar reduction in fipronil desulfinyl formation (relative to total fipronil photodegradation) would be observed in Coastal Plain ("blackwater") regions of the southeastern U.S. where DOM loadings commonly exceed 15 mg/L (*54*).

Acknowledgments

This work was supported by the U.S. Environmental Protection Agency Grant R827397. We would like to extend our gratitude to Dr. G. Thomas Chandler, Department of Environmental Health Science, University of South Carolina, for the use of his GC-ECD. In addition, we would like to Dr. C. J. Murphy, Department of Chemistry and Biochemistry, University of South Carolina, for the use of her UV–vis–NIR spectrophotometer.

Supporting Information Available

Additional tables and figures. This material is available free of charge via the Internet at http://pubs.acs.org.

Literature Cited

(1) Tingle, C. C. D.; Rother, J. A.; Dewhurst, C. F.; Lauer, S.; King, W J. Fipronil: Environmental fate, ecotoxicology, and human health concerns. *Rev. Environ. Contam. Toxicol.* **2003**, *176*, 1–66.

(2) *Fipronil environmental fate and ecological effects assessment and characterization for a section 3 for broadcast treatment with granular product to control turf insects and fire ants (addendum)*; U.S. EPA, Environmental Fate and Effects Division, Office of Pesticides and Toxic Substances, Washington, DC, 2001.

(3) Cole, L. M.; Nicholson, R. A.; Casida, J. E. Action of phenylpyrazole insecticides at the GABA-gated chloride channel. *Pestic. Biochem. Physiol.* **1993**, *46*, 47–54.

(4) Gant, D. B.; Chalmers, A.; Wolff, M.; Hoffman, H.; Bushey, D. Fipronil: action at the GABA receptor. *Rev. Toxicol.* **1998**, *2*, 147–156.

(5) Robinson, T. N.; Olsen, R. W. In *Comparative Invertebrate Neurochemistry*; Lunt, G. G., Olsen, R. W., Eds.; Cornell University Press: Ithaca, NY, 1988; pp 90–123.

(6) Connelly, P. *Environmental Fate of Fipronil*; Environmental Monitoring Branch, Department of Pesticide Regulation, California EPA, Sacramento, CA, 2001.

(7) Schlenk, D.; Huggett, D. B.; Allgood, J.; Bennet, E.; Rimoldi, J. M. Toxicity of fipronil and its degradation products to *Procambarus* sp.: Field and laboratory studies. *Arch. Environ. Contam. Toxicol.* **2001**, *41*, 325–332.

(8) Key, P. B.; Chung, K. W.; Opatkiewicz, A. D.; Wirth, E. F.; Fulton, M. H. Toxicity of the insecticides fipronil and endosulfan to selected life stages of the grass shrimp (*Palaemonetes pugio*). *Bull. Environ. Contam. Toxicol.* **2003**, *70* (3), 533–540.

(9) Volz, D. C.; Wirth, E. F.; Fulton, M. F.; Scott, G. I.; Strozier, E.; Block, D. S.; Ferry, J. L.; Walse, S. S.; Chandler, G. T. Effects of fipronil and chlorpyrifos on endocrine-related endpoints in female grass shrimp (*Palaemonetes pugio*) *Bull. Environ. Contam. Toxicol.* **2003**, *71* (3), 497–503.

(10) Chandler, G. T.; Carey, T. L.; Volz, D. C.; Walse, S. S.; Ferry, J. L.; Klosterhaus, S. L. Fipronil effects on copepod development, fertility, and reproduction: A rapid life-cycle assay in 96-well microplate format. *Environ. Toxicol. Chem.* **2004**, *23* (1), 117–124.

(11) Cary, T. L.; Chandler, G. T.; Volz, D. C.; Walse, S. S.; Ferry, J. L. Phenylpyrazole insecticide fipronil induces male infertility in the estuarine meiobenthic crustacean *Amphiascus tenuiremis*. *Environ. Sci. Technol.* **2004**, *38* (2), 522–528.

(12) Hainzl, D.; Casida, J. E. Fipronil insecticide: Novel photochemical desulfinylation with retention of neurotoxicity. *Proc. Natl. Acad. Sci. U.S.A.* **1996**, *93*, 12764–12767.

(13) Fenet, H.; Beltran, E.; Gadji, B.; Cooper, J. F.; Coste, C. M. Fate of a phenylpyrazole in vegatation and soil under tropical field conditions. *J. Agric. Food Chem.* **2001**, *49*, 1293–1297.

(14) Bobe, A.; Cooper, J. F.; Coste, C. M.; Muller, M. A. Behaviour of fipronil in soil under Sahelian Plain field conditions. *Pestic. Sci.* **1998**, *52*, 275–281.

(15) Zhu, G.; Wu, J.; Liu, Q.; Sun, J. Degradative routes of fipronil in the model paddy field ecosystem. *Nongyaoxue Xuebao* **2000**, *2* (2), 52–56.

(16) Bobe, A.; Meallier, P.; Cooper, J. F.; Coste, C. Kinetics and mechanism of abiotic degradation of fipronil (hydrolysis and photolysis). *J. Agric. Food Chem.* **1998**, *46*, 2834–2839.

(17) Biever, R. C.; Hoberg, J. R.; Jacobson, B.; Dionne, E.; Sulaiman, M.; McCahon, P. Icon rice seed treatment toxicity to crayfish (*Procambarus clarkii*) in experimental rice paddies. *Environ. Toxicol. Chem.* **2003**, *22*, 167–174.

(18) Nigm, K. K.; Crosby, D. G. Abiotic processes influencing fipronil and desthiofipronil dissipation in California, USA, rice fields. *Environ. Toxicol. Chem.* **2001**, *20*, 972–977.

(19) Aajoud, A.; Ravanel, P.; Tissut, M. Fipronil metabolism and dissipation in a simplified aquatic ecosystem. *J. Agric. Food Chem.* **2003**, *51*, 1347–1352.

(20) Nigm, K. K.; Mabury, S. A.; Crosby, D. G. Elucidation of fipronil photodegradation pathways. *J. Agric. Food Chem.* **2000**, *48*, 4661–4665.

(21) Guo, Y.; Jenks, W. S. Photochemistry and photophysics of aromatic sulfoxides. 3. α-Cleavage and the role of the sulfenic ester. *J. Org. Chem.* **1995**, *60*, 5480–5486.

(22) Still, I. W. J. In *The Chemistry of Sulfones and Sulfoxides*; Patai, S., Rappaport, Z., Stirling, C. J. M., Eds.; John Wiley & Sons Ltd.: New York, 1988; pp 873–887.

(23) *EPI Suite*, v3.10 ed.; U.S. EPA, Washington, DC, 2002.

(24) Ying, G. G.; Kookana, R. S. Sorption of fipronil and its metabolites on soils from south Australia. *J. Environ. Sci. Health, Part B* **2001**, *36*, 545–558.

(25) Ramesh, A.; Balasubramanian, M. Kinetics and hydrolysis of fenamiphos, fipronil, and trifluralin in aqueous buffer solutions. *J. Agric. Food Chem.* **1999**, *47*, 3367–3371.

(26) Canonica, S.; Jans, U.; Stemmler, K.; Hoigne, J. Transformation kinetics of phenols in water: Photosensitization by dissolved natural organic material and aromatic ketones. *Environ. Sci. Technol.* **1995**, *29*, 1822–1831.

(27) Canonica, S.; Hoigne, J. Enhanced oxidation of methoxyphenols at micromolar concetration photosensitized by dissolved natural organic material. *Chemosphere* **1995**, *30*, 2365–2374.

(28) Canonica, S.; Freiburghaus, M. Electron-rich phenols for probing the photochemical reactivity of freshwaters. *Environ. Sci. Technol.* **2001**, *35*, 690–695.

(29) Zepp, R. G.; Baughman, G. L.; Schlotzhauer, P. F. Comparison of photochemical behavior of various humic substances in water. 1. Sunlight-induced reactions of aquatic pollutants photosensitized by humic substances. *Chemosphere* **1981**, *10*, 109.

(30) Zepp, R. G.; Schlotzhauer, P. F.; Sink, R. Photosensitzed transformations involving electronic-energy transfer in natural waters—role of humic substances. *Environ. Sci. Technol.* **1985**, *19*, 74.

(31) Hagg, W. R.; Hoigne, J. Singlet oxygen in surface waters. 3. Photochemical formation and steady-state concentrations in various types of waters. *Environ. Sci. Technol.* **1986**, *20*, 341–348.

(32) Zepp, R. G.; Wolfe, N. L.; Baughman, G. L.; Hollis, R. C. Singlet oxygen in natural waters. *Nature* **1977**, *267*, 421–423.

(33) Frimmel, F. H.; Bauer, H.; Putzien, J.; Murasecco, P.; Braun, A. M. Laser flash photolysis of dissolved aquatic humic material and the sensitized production of singlet oxygen. *Environ. Sci. Technol.* **1987**, *21*, (6), 541–545.

(34) Hagg, W. R.; Hoigne, J.; Gassman, E.; Braun, A. M. Singlet oxygen in surface waters—Part I: Furfuryl alcohol as a trapping agent—Part II: Quantum yields of its production by some natural humic materials as a function of wavelength. *Chemosphere* **1984**, *13*, 631–650.

(35) Brezonik, P. L.; Fulkerson-Brekken, J. Nitrate-induced photolysis in natural waters: Controls on concentrations of hydroxyl radical photointermediates by natural scavenging agents. *Environ. Sci. Technol.* **1998**, *32*, 3004–3010.

(36) Vaughan, P. P.; Blough, N. V. Photochemical formation of hydroxyl radical by constituents of natural waters. *Environ. Sci. Technol.* **1998**, *32* (2), 2947–2953.

(37) Zepp, R. G.; Hoigne, J.; Bader, H. Nitrate-induced photooxidation of trace organic chemicals in water. *Environ. Sci. Technol.* **1987**, *21*, 443−450.
(38) Mill, T.; Hendry, D. G.; Richardson, H. Free-radical oxidants in natural waters. *Science* **1980**, *207*, 886−887.
(39) Torrents, A.; Anderson, B. G.; Bilboulian, S.; Johnson, W. E.; Hapeman, C. J. Atrazine photolysis: mechanistic investigations of direct and nitrate-mediated hydroxyl radical processes and the influence of dissolved organic carbon from the Chesapeake Bay. *Environ. Sci. Technol.* **1997**, *31*, 1476−1482.
(40) Lindsey, M. E.; Tarr, M. A. Inhibiton of hydroxyl radical reaction with aromatics by dissolved natural organic matter. *Environ. Sci. Technol.* **2000**, *34*, 444−449.
(41) Huang, J.; Mabury, S. A. The role of carbonate radical in limiting the persistence of sulfur-containing chemicals in sunlit natural waters. *Chemosphere* **2000**, *41* (11), 1775−1782.
(42) Huang, J.; Mabury, S. A. A new method for measuring carbonate radical reactivity toward pesticides. *Environ. Toxicol. Chem.* **2000**, *19* (6), 2181−2188.
(43) Larson, R. A.; Zepp, R. G. Reactivity of the carbonate radical with aniline derivatives. *Environ. Toxicol. Chem.* **1988**, *7*, 265−274.
(44) Faust, B. C.; Hoigne, J. Sensitized photooxidation of phenols by fulvic acid and in natural waters. *Environ. Sci. Technol.* **1987**, *21*, 957−964.
(45) Draper, W. M.; Crosby, D. G. Hydrogen-peroxide and hydroxyl radical—intermediates in indirect photolysis reaction in water. *J. Agric. Food Chem.* **1981**, *29* (4), 699.
(46) Draper, W. M.; Crosby, D. G. Solar photooxidation of pesticides in dilute hydrogen-peroxide. *J. Agric. Food Chem.* **1984**, *32* (2), 231.
(47) Fischer, A. M.; Kilger, D. S.; Winterle, J. S.; Mill, T. Direct observation of phototransients in natural waters. *Chemosphere* **1985**, *14*, 1299.
(48) Zepp, R. G.; Braun, A. M.; Hoigne, J.; Leenheer, J. A. Photoproduction of hydrated electrons from natural organic solutes in aquatic environments. *Environ. Sci. Technol.* **1987**, *21*, 485.
(49) Zafiriou, O. C.; Joussot-Dubien, J.; Zepp, R. G.; Zika, R. G. Photochemistry of natural waters. *Environ. Sci. Technol.* **1984**, *18* (12), 358A.
(50) Cooper, W. J.; Zika, R. G. Photochemical formation of hydrogen-peroxide in surface and groundwaters exposed to sunlight. *Science* **1983**, *220*, 771.
(51) Draper, W. M.; Crosby, D. G. The photochemical generation of hydrogen-peroxide in natural waters. *Arch. Environ. Contam. Toxicol.* **1983**, *12* (1), 121.
(52) Miller, P. L.; Chin, Y. P. Photoinduced degradation of carbaryl in a wetland surface water. *J. Agric. Food Chem.* **2002**, *50*, 6758−6765.
(53) Lam, M. W.; Tantuco, K.; Mabury, S. A. Photofate: A new approach in accounting for the conribution of indirect photolysis of pesticides and pharmaceuticals in surface waters. *Environ. Sci. Technol.* **2003**, *37*, 899−907.
(54) Harrison, J. *STORET*; U.S. EPA, Washington, DC, www.epa.gov/STORET/dbtop.html (accessed May 2002).
(55) Walse, S. S.; Scott, G. I.; Ferry, J. L. Stereoselective degradation of aqueous endosulfan in modular estuarine mesocosms: identification of endosulfan γ-hydroxycarboxylate. *J. Environ. Monit.* **2003**, *5* (3), 373−379.
(56) Walse, S. S.; Pennington, P.; Scott, G. I.; Ferry, J. L. The fate of fipronil in modular estuarine mesocosms. *J. Environ. Monit.* **2004**, *6* (1), 58−64
(57) Lauth, J. R.; Scott, G. I.; Cherry, D. S.; Buikema, A. L. J. A modular estuarine mesocosm. *Environ. Toxicol. Chem.* **1996**, *15* (5), 630−637.
(58) Pennington, P. L. Ph.D. Thesis, School of Public Health, University of South Carolina, Columbia, SC, 2002.
(59) DeLorenzo, M. E.; Lauth, J.; Pennington, P. L.; Scott, G. I.; Ross, P. E. Atrazine effects on the microbial food web in tidal creek mesocosms. *Aquat. Toxicol.* **1999**, *46* (3−4), 241−251.
(60) Taylor, H. A. In *Analytical Photochemistry and Photochemical Analysis*; Fitzgerald, J. M., Ed.; Marcel Dekker: New York, 1971; pp 109−111.
(61) Montgomery, D. C. *Design and Analysis of Experiments*, 5th ed.; John Wiley & Sons: New York, 2001.
(62) Deming, S. N.; Morgan, S. L. *Experimental Design: A Chemometric Approach*, 2nd ed.; Elseiver Science Publishers B. V.: Amsterdam, 1993.
(63) Demcheck, D. K.; Skrobialowski, S. C. *Fipronil and degradation products in the rice-producing areas of the Mermentau River Basin, Louisiana, February-September 2000*; U. S. Geological Survey, 2003.
(64) Kong, L.; Ferry, J. L. Effect of salinity on the photolysis of chrysene adsorbed to a smectite clay. *Environ. Sci. Technol.* **2003**, *37* (21), 4894−4900.
(65) Walse, S. S.; Shimizu, K. D.; Ferry, J. L. Surface-catalyzed transformations of aqueous endosulfan. *Environ. Sci. Technol.* **2002**, *36* (22), 4846−4853.
(66) Calvert, J. G.; Pitts, J. R. In *Photochemistry*; Wiley: New York, 1967; pp 781−783.
(67) Leifer, A. *The Kinetics of Environmental Aquatic Photochemistry: Theory and Practice*; American Chemical Society: Washington, DC, 1988.
(68) Zepp, R. G. Quantum yields for reaction of pollutants in dilute aqueous solution. *Environ. Sci. Technol.* **1978**, *12*, 327−329.
(69) Weber, E. J.; Spidle, D. L.; Thorn, K. A. Covalent binding of aniline to humic substances. 1. Kinetic studies. *Environ. Sci. Technol.* **1996**, *30*, 2755−2763.
(70) Miller, G. C.; Zepp, R. G. Photoreactivity of aquatic pollutants sorbed on suspended sediments. *Environ. Sci. Technol.* **1979**, *13*, 860−863.
(71) Miller, G. C.; Zepp, R. G. Effects of suspended sediments on photolysis rates of dissolved pollutants. *Water Res.* **1979**, *13*, 453−459.
(72) Skurlatov, Y. L.; Zepp, R. G.; Baughman, G. L. Photolysis rates of (2,4,5-trichlorophenoxy) acetic acid and 4-amino-3,5,6-trichloropicolinic acid in natural waters. *J. Agric. Food Chem.* **1983**, *31*, 1065−1071.
(73) Miller, G. C.; Zisook, R.; Zepp, R. G. Photolysis of 3,4-dichloroaniline in natural waters. *J. Agric. Food Chem.* **1980**, *28*, 1053−1056.
(74) Balzani, V.; Carassiti, V. *Photochemistry of Coordination Compounds*; Academic: New York, 1970; Chapter 2.
(75) Jankowski, J. J.; Kieber, D. J.; Mopper, K. Nitrate and nitrite ultraviolet actinometers. *Photochem. Photobiol.* **1999**, *70* (3), 319−328.
(76) Schlautman, M. A.; Morgan, J. J. Effects of aqueous chemistry on the binding of polycyclic aromatic hydrocarbons by dissolved humic materials. *Environ. Sci. Technol.* **1993**, *27*, 961−969.
(77) Engebreston, R. R.; Wandruszka, R. v. Microorganization in dissolved humic acids. *Environ. Sci. Technol.* **1994**, *28*, 1934−1941.
(78) Gauthier, T. D.; Seitz, W. R.; Grant, C. L. Fluorescence quenching mechanism for determining equilibrium constants for polycyclic aromatic hydrocarbons binding to dissolved humic materials. *Environ. Sci. Technol.* **1986**, *20* (11), 1162−1166.
(79) Kumke, M. U.; Lohmannsroben, H. G.; Roch, T. Fluorescence quenching of polycyclic aromatic compounds by humic acid. *Analyst* **1994**, *119*, 997−1001.
(80) Backus, D. A.; Gschwend, P. M. Fluorescent polycyclic aromatic hydrocarbons as probes for studying the impact of colloids on pollutant transport in groundwater. *Environ. Sci. Technol.* **1990**, *24*, 1214−1223.
(81) Doll, T. E.; Frimmel, F. H.; Kumke, M. U. Interaction between matural organic matter (NOM) and polycyclic aromatic compounds (PAC)—comparison of fluorescence quenching and solid-phase micro extraction (SPME). *Fresenius' J. Anal. Chem.* **1999**, *364*, 313−319.
(82) Karickhoff, S. W. Semiempirical estimation of sorption of hydrophobic pollutants on natural sediments and soils. *Chemosphere* **1981**, *10* (8), 833−846.
(83) Wenska, G. Quenching of the fluorescence of naphthalene derivatives by nucleic acid components. *Pol. J. Chem.* **1997**, *71*, 797−806.
(84) Muller, M. B.; Vercammen, K.; Frimmel, F. H. Interactions between ofloxacin and NOM investigated by fluorescence quenching technique. *Vom Wasser* **2003**, *100*, 85.
(85) *Humic Substances in Terrestrial Ecosystems*; Piccolo, A., Ed.; Elsevier Science: New York, 1996.
(86) Stevenson, F. J. *Humus Chemistry: Genesis, Composition, Reactions*; John Wiley & Sons: New York, 1994.
(87) Zepp, R. G.; Cline, D. M. Rates of direct photolysis in aquatic enviroment. *Environ. Sci. Technol.* **1977**, *11*, 359−366.

Received for review August 15, 2003. Revised manuscript received April 27, 2004. Accepted May 4, 2004.

ES0349047